

# Anisotropic splitting and spin polarization of metallic bands due to spin-orbit interaction at the Ge(111)( $\sqrt{3} \times \sqrt{3}$ )R30°-Au surface

Kan Nakatsuji,<sup>\*</sup> Ryota Niikura, Yuki Shibata, Masamichi Yamada, Takushi Iimori, and Fumio Komori<sup>†</sup>  
*Institute for Solid State Physics, University of Tokyo, 5-1-5 Kashiwanoha, Kashiwa-shi, Chiba 277-8581, Japan*

Yasuhiro Oda and Akira Ishii

*Department of Applied Mathematics and Physics, Tottori University, 4-101 Minami, Koyama, Tottori 680-8552, Japan*

(Received 21 February 2011; revised manuscript received 30 April 2011; published 26 July 2011)

Valence electronic structure of the Ge(111)( $\sqrt{3} \times \sqrt{3}$ )R30°-Au surface was studied by angle-resolved photoemission spectroscopy and density functional calculations. Two metallic surface bands were observed around  $\bar{\Gamma}$ , and parts of them split into spin-polarized bands owing to the spin-orbit interaction. One is a holelike band and originates only from the Ge atoms. The other is an electronlike band and is made of the surface Au and Ge atoms. The polarized spin in these bands has the component normal to the surface as well as that parallel to the surface. These results are attributed to spin-orbit interaction in a large and anisotropic potential gradient at this surface.

DOI: [10.1103/PhysRevB.84.035436](https://doi.org/10.1103/PhysRevB.84.035436)

PACS number(s): 73.20.At, 79.60.Jv, 73.61.Cw

## I. INTRODUCTION

Spin-polarized metallic surface states at semiconductor surfaces have attracted much attention for the study of the spin-polarized two-dimensional electron transport and its applications to spin-dependent electronics.<sup>1</sup> One of the promising ways to realize the spin-polarized surface state is the use of strong spin-orbit coupling, called the Rashba effect.<sup>2</sup> So far, however, such splitting of the metallic surface state has been reported only on a Pb-adsorbed Ge(111) surface.<sup>3</sup> It is known that metal adsorbed group IV semiconductors often have metallic surface electronic bands with ( $\sqrt{3} \times \sqrt{3}$ )R30° surface structures. Among them, we focus on the Au-adsorbed Ge(111) surface with two metallic bands<sup>4</sup> because a heavy element such as Au can induce a large Rashba effect.

The strength of the spin-orbit interaction depends on the potential gradient for the electrons, and thus the surface structure largely affects the splitting of the spin-polarized bands. For metal surfaces, correlation among the elements, surface structure, and splitting of the spin-polarized bands has been discussed.<sup>5</sup> Similarly, on the semiconductor surfaces, the structure largely affects the direction and magnitude of the spin polarization of the surface bands. The structure of the Au-adsorbed Ge(111) surface is well expressed using a conjugate honeycomb-chained-trimer (CHCT) model according to previous studies by x-ray and low-energy electron diffraction (LEED).<sup>6,7</sup> In this model, monolayer Au atoms form trimers on the surface, and the potential gradient at the surface is not simply surface normal but depends on the details of local arrangement of the surface atoms.

In the present study, we have investigated the valence surface states of the Ge(111) ( $\sqrt{3} \times \sqrt{3}$ )R30°-Au surface using angle-resolved photoemission spectroscopy (ARPES) and density functional calculations. Both electronlike and holelike bands were found to create the Fermi surfaces around  $\bar{\Gamma}$  in the previous ARPES study,<sup>4</sup> while the detailed band structure has not been clarified. We compare the experimental results with the calculated electronic structure including the spin-orbit interaction for an optimized CHCT structure. The observed splitting of the parts of the metallic bands is attributed

to anisotropic Rashba splitting in the large potential gradient of this surface structure. Spin polarization of the surface bands is confirmed in the calculation.

## II. METHODS

The surface was studied by ARPES in two independent chambers. The spectra were measured with 21.2-eV nonpolarized and polarized photons using a He discharged lamp and with 33-eV polarized photons at BL18A of Photon Factory, High Energy Accelerator Research Organization (KEK), in Tsukuba. The photoelectrons were collected by hemispherical analyzers. For the band mapping, a two-dimensional detector was used. The chamber with the lamp was equipped with an Al-K $\alpha$  x-ray source for x-ray photoemission spectroscopy (XPS). The symmetry of the surface bands were experimentally studied using *s*- and *p*-polarized photons of 21.2 eV. The polarization dependence of the photoemission intensity was recorded along the  $\bar{\Gamma}$ - $\bar{K}$  line of the  $\sqrt{3} \times \sqrt{3}$  surface Brillouin zone (SBZ), which is included in a mirror plane of the surface. Spectra were measured at room temperature (RT) and 130 K. No significant difference was observed in the ARPES spectra except thermal broadening.

The base pressure of the sample-preparation and measurement chambers was less than  $1 \times 10^{-8}$  Pa. Substrates of *n*-type Ge(111) were cleaned by repeated cycles of 1-keV Ar<sup>+</sup> ion sputtering at 675 K and resistive heating up to 1050 K for 1 min and 950 K for 15 min. The cleanliness of the surface was confirmed by the absence of XPS signals from contaminants.

Gold was deposited from a tungsten basket onto the clean surface kept at 675 K. The deposition rate of Au was monitored by a quartz microbalance and calibrated by the intensity ratio of Au 4*f* and Ge 2*p* core level spectra as in the previous report.<sup>4</sup> The Au deposition rate on the surface was 0.5–1 monolayer (ML) / min. Here, ML is defined as the same number density of atoms as that on the ideal Ge(111)  $1 \times 1$  surface. At BL18A, the 1-ML Au coverage was determined by the appearance of  $16 \times$  spots in the LEED pattern on the Ge(001)-Au surface. This Au coverage corresponds to 1 ML on the Ge(111) substrate.<sup>4</sup>

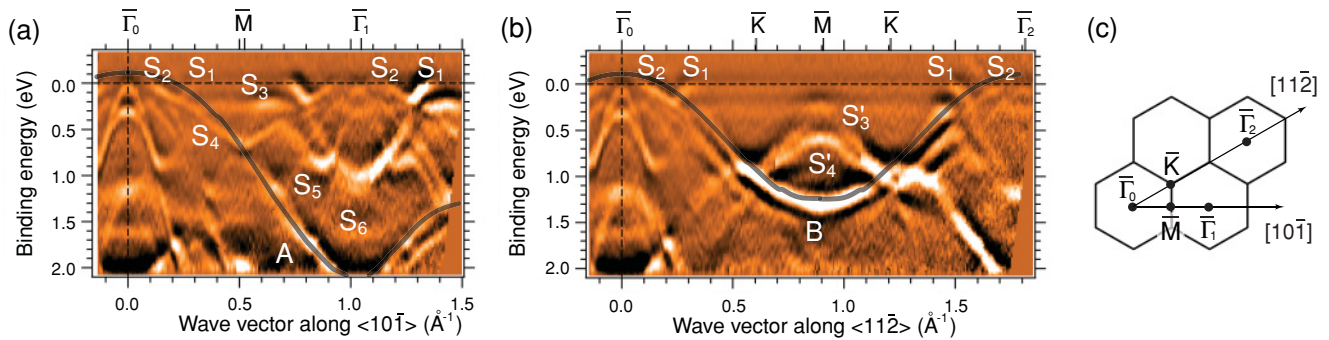


FIG. 1. (Color online) Observed valence band structure of the Ge(111)( $\sqrt{3} \times \sqrt{3}$ )R30 $^\circ$ -Au surface at RT in the  $\langle 10\bar{1} \rangle$  (a) and  $\langle 11\bar{2} \rangle$  (b) directions. The origin of the energy is the Fermi energy  $E_F$ . The second derivative of the spectra is plotted, and the bright areas indicate the positions with high photoemission intensity. The Au coverage was 1 ML on average. The  $S_1$ – $S_6$ ,  $S'_3$ , and  $S'_4$  bands are identified as surface states, and the A and B bands are as bulk states. Solid curves indicate the band edges of the projected bulk electronic states in the both directions.<sup>15–17</sup> (c) SBZ of the  $\sqrt{3} \times \sqrt{3}$  surface.

Our first-principles total-energy calculations are based on the density functional theory (DFT)<sup>8,9</sup> using the VIENNA *ab initio* SIMULATION PACKAGE (VASP).<sup>10</sup> We used the local density approximation<sup>9,11</sup> for the exchange correlation and projector augmented wave (PAW)<sup>12,13</sup> potentials. The cutoff energy for the plane-wave basis is set to be 312.5 eV. We employed supercells containing eighteen atomic layers of Ge and a vacuum region of 2.0 nm. The bottom layer of the slab is passivated with hydrogen atoms. The Ge atoms of the nine layers on this side of the slab are kept fixed, and all other atoms are allowed to relax in order to simulate the constraint coming from the underlying semi-infinite bulk. In the calculations of the optimized atomic structure and band structure,  $k$  points are applied meshes of  $4 \times 4 \times 1$  and  $8 \times 8 \times 1$  points, respectively. We calculated the *spd*- and site-projected wave-function character of each band by using a quick projection scheme with the PAW method under the default setting of VASP.<sup>14</sup>

### III. RESULTS AND DISCUSSION

The valence-band photoemission spectra of the Ge(111)( $\sqrt{3} \times \sqrt{3}$ )R30 $^\circ$ -Au surface at RT using 21.2-eV photons are shown in Figs. 1(a) and 1(b). The SBZ of the  $\sqrt{3} \times \sqrt{3}$  surface is given in Fig. 1(c). The positions of the projected bulk band edges shown as solid curves in Figs. 1(a) and 1(b) are determined by comparing the subsurface and bulk bands with both the previous ARPES results<sup>15,16</sup> for the clean and H-adsorbed surfaces and the results<sup>17</sup> of band calculations. The bands labeled A and B in Figs. 1(a) and 1(b) are identified as bulk bands since they are commonly detected in the both present and H-adsorbed surfaces and trace the bulk band edges. The energy positions of all the detected bulk bands are 0.3 eV higher than those in the clean and H-adsorbed surfaces. The 0.3-eV energy shift of the Ge bulk component was previously reported in the Ge 3*d* core level.<sup>18</sup> This is ascribed to the surface band bending and makes the top of the bulk valence band 0.1 eV higher than the Fermi energy  $E_F$  as in Figs. 1(a) and 1(b). The large density of surface acceptor states induces such a large band bending.

We identified the surface bands characteristic to the Ge(111)( $\sqrt{3} \times \sqrt{3}$ )R30 $^\circ$ -Au surface,  $S_1$ – $S_6$ , as indicated in

Fig. 1(a). These are found in the bulk band gap and have never been observed in the clean and H-adsorbed surfaces. Around  $\bar{\Gamma}_1$  in the bulk band gap, two surface bands clearly cross  $E_F$ . One is the electronlike  $S_1$  band, and the other the holelike  $S_2$ . Intensity of the former band increased using 33-eV photons, while the latter band was not detected in this case. The bottom of the  $S_1$  band is 1 eV below  $E_F$ . The dispersions along the  $\bar{K}$ – $\bar{M}$  line for the  $S_3$  and  $S_4$  bands are shown in Fig. 1(b) as  $S'_3$  and  $S'_4$ . The result of the Fermi surface mapping around  $\bar{\Gamma}_1$  on this surface was given in Ref. 4. Both  $S_1$  and  $S_2$  bands show a sixfold symmetry, in contrast to the round Fermi surface for the Si(111)-Au<sup>19</sup> and Si(111)-Ag<sup>20</sup> surfaces.

Figures 2(a) and 2(b) show the results of high-resolution ARPES beyond  $\bar{\Gamma}_1$  of the second SBZ close to  $E_F$  at 130 K. A holelike band,  $S'_2$ , exists 70 meV below the  $S_2$  band in the binding energy ( $E_B$ ) range between 0.3 and 0 eV. It almost touches  $E_F$  near  $\bar{\Gamma}_1$ . For the  $S_1$  band, a split band of 60 meV,  $S'_1$ , is noticeable between  $E_B = 0.2$  and 0 eV while the band is single below  $E_B = 0.2$  eV. The open circles on the  $S_1$  and

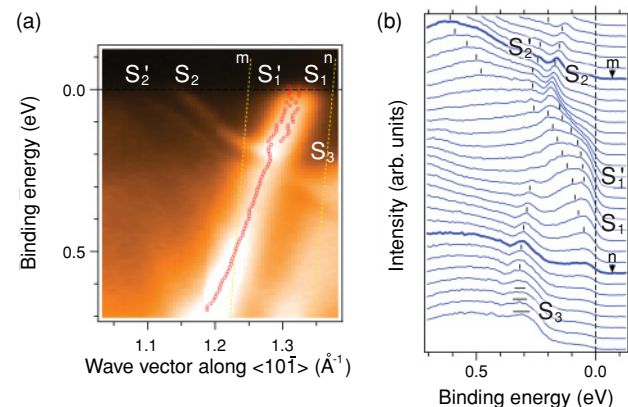


FIG. 2. (Color online) Energy dispersion by the photoemission intensity plot (a) and corresponding spectra (b) of the Ge(111)( $\sqrt{3} \times \sqrt{3}$ )R30 $^\circ$ -Au surface at 130 K beyond  $\bar{\Gamma}_1$  in the  $\langle 10\bar{1} \rangle$  direction. The two spectra labeled by small arrows (m and n) in (b) were recorded along the dotted lines (m and n) in (a). In (a), peak positions of MDC are plotted by open (red) circles for the  $S_1$  and  $S'_1$  bands. The spectral line width of the  $S_3$  band is broad for large wave vectors as indicated in (b).

$S'_1$  bands in Fig. 2(a) are the peak positions of the momentum distribution curves (MDCs). The spectral line width of the  $S_3$  band becomes broad with increasing the wave vector, as shown in Fig. 2(b).

In Fig. 3, we show the calculated band structure. The origin of energy is determined by the charge neutrality of the whole slab and does not always agree with the observed  $E_F$  because of the band bending in the experiments. The optimized surface structure<sup>21</sup> is almost the same as the CHCT model obtained by LEED.<sup>7</sup> The surface consists of the Au trimers and Ge atoms as schematically shown in Fig. 3(b). There is only one electronlike band around  $\bar{\Gamma}$ , and the observed  $S_1$  band is assigned as this band. On the other hand, there are several holelike bands around  $\bar{\Gamma}$ .

To understand the origins of the observed bands, we theoretically analyzed the charge distribution and symmetry of the bands. We find that the  $S_1$  band originates from the Au trimers and the surface Ge atoms in the CHCT model. In

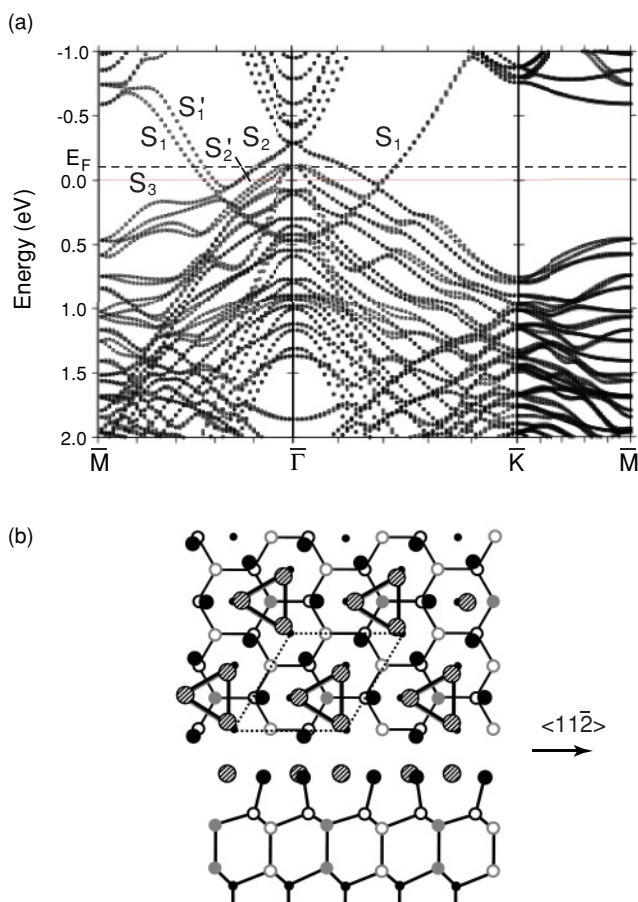


FIG. 3. (a) Calculated band structure of the Ge(111)( $\sqrt{3} \times \sqrt{3}$ )R30 $^\circ$ -Au surface. Some of the surface states are identified. The origin of energy is determined by the charge neutrality of the whole slab. The Fermi energy determined by comparing the calculated bands with the observed Fermi surface is shown as a dashed line indicating  $E_F$ . (b) Top and side views of a schematic atomic model of the CHCT model. The dotted rhombus shows a  $\sqrt{3} \times \sqrt{3}$  unit cell. The gold trimer is indicated by hatched balls and thick sticks. Larger solid balls are the surface Ge atoms. Subsurface Ge atoms are represented by other small balls.

TABLE I. Polarization dependence of the surface bands observed in the  $\bar{\Gamma}_0$ - $\bar{K}$ - $\bar{M}$  direction.  $\circ$ , observed;  $\times$ , not observed.

Band	$S_1$		$S_2$		$S'_3$	$S'_4$
	$\bar{\Gamma}_0$	$\bar{\Gamma}_2$	$\bar{\Gamma}_0$	$\bar{\Gamma}_2$		
$s$ -polarization	$\circ$	$\circ$	$\circ$	$\times$	$\times$	$\times$
$p$ -polarization	$\times$	$\times$	$\circ$	$\circ$	$\circ$	$\circ$

contrast, the highest holelike band originates from the surface and subsurface Ge atoms with little contribution from the Au trimer, and the second highest only from the subsurface Ge atoms. These two bands should be observed by ARPES, and thus the highest holelike band can be identified as  $S_2$  and the second highest as  $S'_2$ . The broad feature of the  $S_3$  band observed close to  $\bar{M}$  in the  $\bar{\Gamma}$ - $\bar{M}$  direction are identified as the first and second highest occupied bands at the same position in the calculation.

We compare the band symmetry observed in the experiment with the results of the calculation. In Table I, we summarize the polarization dependence of the surface bands observed in the  $\bar{\Gamma}_0$ - $\bar{K}$ - $\bar{M}$  direction (mirror plane). The  $S_1$  band was observed only by the  $s$ -polarized light, suggesting its odd symmetry and in-plane character. This is consistent with the results of the band calculation;  $S_1$  mainly consists of in-plane  $p$  and  $d$  orbitals. The  $S_2$  and  $S'_2$  bands were observed by the both polarizations, suggesting their different symmetries from that of the  $S_1$  band. In the calculation, not only the in-plane orbitals but also the out-of-plane  $p_z$  orbital have significant contribution to the  $S_2$  and  $S'_2$  bands. Other surface state bands,  $S'_3$  and  $S'_4$ , have even symmetry to the mirror plane since they were observed only by the  $p$ -polarized light.

For qualitative comparison between the calculated bands and the experimental results, the band bending should be considered in the calculation by shifting the bands down in the energy axis direction. Here, we set  $E_F = -0.1$  eV in Fig. 3 to reproduce the shape of the observed Fermi surface qualitatively. In the calculation, the Fermi wave vector ( $k_F$ ) of the  $S_2$  band in the  $\bar{\Gamma}$ - $\bar{M}$  direction is smaller than that in the  $\bar{\Gamma}$ - $\bar{K}$  direction. This is consistent with the observed anisotropic Fermi surface.<sup>4</sup> On the other hand,  $k_F$  of the  $S_1$  band in the calculation is almost the same in the both directions, contrary to the observation of Fermi surface. The sixfold appearance of the Fermi surface should be due to the existence of the  $S'_1$  band only in the  $\bar{\Gamma}$ - $\bar{M}$  direction.

The 0.1-eV shift of the calculated bands, however, does not remove the discrepancy on the position of the  $S_1$  band bottom between the experiment and calculation; it is still deeper in the experiment. In addition, there remain quantitative differences in the surface bands between them. For example, the  $S_1$  band clearly splits into two bands in the  $\bar{\Gamma}$ - $\bar{M}$  direction above the crossing point with the  $S_2$  band both in the experiment and the calculation. The separation at  $E_F$  is, however, about 60 meV in Fig. 2 while it is 100 meV in the calculation. These suggest that the surface atomic structure should be more quantitatively optimized in the calculation.

We analyzed the spin polarization of the  $S_1$  and  $S'_1$  bands in the calculation and confirmed these are spin-split bands. It is noted that both in-plane and out-of-plane spin components

are opposite in these two bands. The split is absent in the calculation without spin degree of freedom. Thus, we conclude this is due to spin-orbit interaction. Very small spin splitting of the  $S_1$  band can be seen in the  $\bar{\Gamma}$ - $\bar{M}$  direction below the crossing point with the  $S_2$  band and in the  $\bar{\Gamma}$ - $\bar{K}$  direction. These results qualitatively agree with the observation that the splitting of the  $S_1$  band is significant only in the  $\bar{\Gamma}$ - $\bar{M}$  direction above the crossing point with the  $S_2$  band. In the other part of the  $S_1$  band, the band split was not detected with the energy resolution of the present ARPES measurements, 35 meV.

It is natural that the  $S_1$  band originating from the surface Au atoms show a Rashba splitting. Generally, a heavy element such as Au has a large spin-orbit interaction, and a Rashba splitting in a large potential gradient is expected at the surface. However, a simple consideration on the splitting for two-dimensional electrons is not applicable to the present system. Significant splitting of the  $S_1$  band appears only in a limited area of the  $k$  space around the  $\bar{\Gamma}$ - $\bar{M}$  direction above the crossing point with the  $S_2$  band. Moreover, the polarized spin has a surface-normal component. These results are in contrast to the reported metallic band in the Pb-adsorbed Ge(111) surface,<sup>3</sup> where the Rashba splitting was isotropic around  $\bar{\Gamma}$ . The direction of the surface electric field and thus the spin polarization of the metallic bands are more complicated in the present system of the CHCT structure than those in a flat  $\beta(\sqrt{3} \times \sqrt{3})$  structure<sup>22</sup> of the Pb-adsorbed Ge(111) surface.

The spin-orbit interaction also induces spin polarization in the other electronic states. In the calculation, the  $S_2$  and  $S'_2$  bands originating mainly from the Ge  $4s$  and  $4p$  states are spin polarized with both in-plane and out-of-plane spin components. The spin polarization in the both bands is large when the in-plane wave vector is between 0.1 and 0.2  $\text{\AA}^{-1}$ . These bands resemble the two spin-polarized holelike bands due to subsurface Ge atoms reported on the Bi-adsorbed Ge(111) surface.<sup>23</sup> A spin-polarized band of metal-adsorbed Ge(111) surface does not always originate from the surface heavy elements.

In Fig. 3(a), the  $S_3$  band in the  $\bar{\Gamma}$ - $\bar{M}$  direction splits into two bands below 0.2 eV. Correspondingly, in Fig. 2, the  $S_3$  band in the  $\bar{\Gamma}$ - $\bar{M}$  direction becomes broad when the wave vector increases while the splitting is not obvious. These are spin polarized and consist partly of the surface Au and Ge atoms in the calculation. Both in-plane and out-of-plane spin components are polarized as in the  $S_1$  and  $S'_1$  bands. The spin-orbit interaction at the present surface of Au and Ge atoms makes the spin-dependent electronic structure anisotropic and complicated. Varieties of the spin splitting of the valence bands among Au-, Pb-,<sup>3</sup> and Bi-adsorbed<sup>23</sup> Ge(111) surfaces are attributed to differences in the surface atomic structure.

#### IV. CONCLUSION

We have studied the surface electronic structure of Ge(111)( $\sqrt{3} \times \sqrt{3}$ ) $R30^\circ$ -Au by both ARPES and the calculations based on DFT. Two metallic bands around  $\bar{\Gamma}$ ,  $S_1$  and  $S_2$ , are spin polarized at  $E_F$  in different ways. The former is an electronlike band originating from the surface Au and Ge atoms. This shows Rashba splitting above  $E_B = 0.2$  eV in the  $\bar{\Gamma}$ - $\bar{M}$  direction while no splitting was observed in the  $\bar{\Gamma}$ - $\bar{K}$  direction. The latter band is a holelike band originating only from Ge atoms and shows spin polarization. The occupied  $S'_2$  and  $S_3$  bands are also spin polarized. These spin-polarized bands are attributed to the spin-orbit interaction of the CHCT structure with anisotropic potential gradient at the surface.

#### ACKNOWLEDGMENTS

The authors greatly acknowledge Koichiro Yaji for fruitful discussions. They also thank Ayumi Harasawa for her collaboration at the Photon Factory (PF-PAC No. 2008G663). The present work was partly supported by Grant-in-Aid for Scientific Research (A) 21244048 and Grant-in-Aid for Young Scientists (B) 22710095 from JSPS. It was also partly supported by a grant-in-aid from the NSG Foundation.

\*nakatsuji@issp.u-tokyo.ac.jp

<sup>†</sup>komori@issp.u-tokyo.ac.jp

<sup>1</sup>I. Zutic, J. Fabian, and S. Das Sarma, *Rev. Mod. Phys.* **76**, 323 (2004).

<sup>2</sup>Yu. A. Bychkov and È. I. Rashba, *Pis'ma Zh. Eksp. Teor. Fiz.* **39**, 66 (1984) [*JETP Lett.* **39**, 78 (1984)].

<sup>3</sup>K. Yaji, Y. Ohtsubo, S. Hatta, H. Okuyama, K. Miyamoto, T. Okuda, A. Kimura, H. Namatame, M. Taniguchi, and T. Aruga, *Nature Commun.* **1**, 17 (2010).

<sup>4</sup>K. Nakatsuji, R. Niikura, Y. Shibata, M. Yamada, T. Iimori, and F. Komori, *Phys. Rev. B* **80**, 081406(R) (2009).

<sup>5</sup>I. Gierz, B. Stadtmüller, J. Vuorinen, M. Lindroos, F. Meier, J. H. Dil, K. Kern, and C. R. Ast, *Phys. Rev. B* **81**, 245430 (2010).

<sup>6</sup>P. B. Howes, C. Norris, M. S. Finney, E. Vlieg, and R. G. van Silfhout, *Phys. Rev. B* **48**, 1632 (1993).

<sup>7</sup>H. Over, C. P. Wang, and F. Jona, *Phys. Rev. B* **51**, 4231 (1995).

<sup>8</sup>P. Hohenberg and W. Kohn, *Phys. Rev.* **136**, B864 (1964).

<sup>9</sup>W. Kohn and L. J. Sham, *Phys. Rev.* **140**, A1133 (1965).

<sup>10</sup>G. Kresse and J. Furthmüller, *Phys. Rev. B* **54**, 11169 (1996).

<sup>11</sup>J. P. Perdew and Y. Wang, *Phys. Rev. B* **33**, 8800 (1986).

<sup>12</sup>P. E. Blöchl, *Phys. Rev. B* **50**, 17953 (1994).

<sup>13</sup>G. Kresse and D. Joubert, *Phys. Rev. B* **59**, 1758 (1999).

<sup>14</sup>G. Kresse and J. Furthmüller, [<http://cms.mpi.univie.ac.at/vasp/>].

<sup>15</sup>I. Razado Colombo, J. He, H. M. Zhang, G. V. Hansson, and R. I. G. Uhrberg, *Phys. Rev. B* **79**, 205410 (2009).

<sup>16</sup>I. Razado Colombo, H. M. Zhang, and R. I. G. Uhrberg, *Phys. Rev. B* **80**, 193403 (2009).

<sup>17</sup>S. Hatta, T. Aruga, C. Kato, S. Takahashi, H. Okuyama, A. Harasawa, T. Okuda, and T. Kinoshita, *Phys. Rev. B* **77**, 245436 (2008).

<sup>18</sup>M. Göthelid, M. Hammar, M. Björkqvist, U. O. Karlsson, S. A. Flodström, C. Wigren, and G. LeLay, *Phys. Rev. B* **50**, 4470 (1994).

<sup>19</sup>H. M. Zhang, T. Balasubramanian, and R. I. G. Uhrberg, *Phys. Rev. B* **66**, 165402 (2002).

<sup>20</sup>L. S. O. Johansson, E. Landemark, C. J. Karlsson, and R. I. G. Uhrberg, *Phys. Rev. Lett.* **63**, 2092 (1989).

<sup>21</sup>Y. Oda and A. Ishii (unpublished).

<sup>22</sup>S. A. de Vries, P. Goettkindt, P. Steadman, and E. Vlieg, *Phys. Rev. B* **59**, 13301 (1999).

<sup>23</sup>Y. Ohtsubo, S. Hatta, K. Yaji, H. Okuyama, K. Miyamoto, T. Okuda, A. Kimura, H. Namatame, M. Taniguchi, and T. Aruga, *Phys. Rev. B* **82**, 201307(R) (2010).